Figure S1.

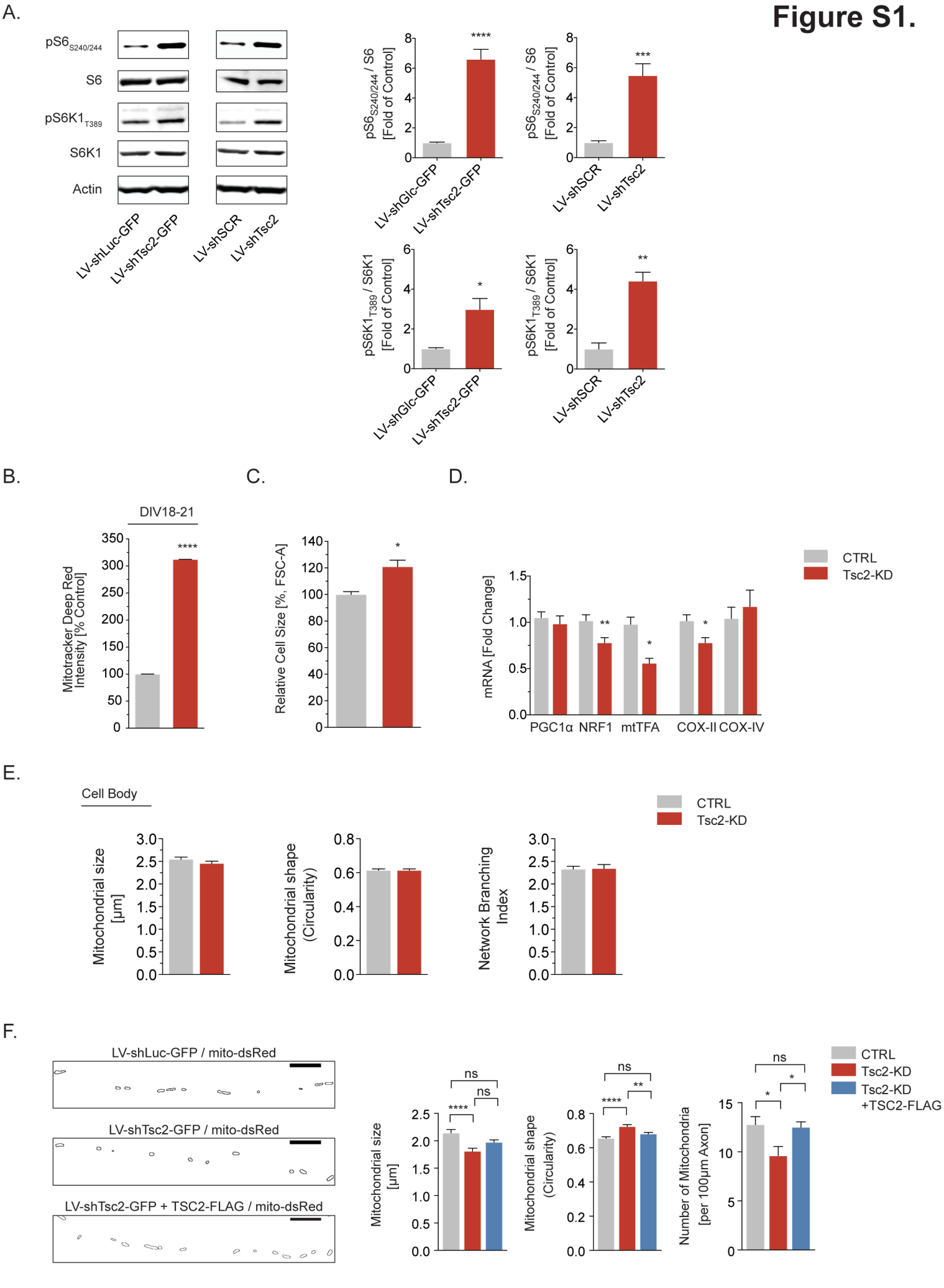
A.
pS6S240/244
S6
pS6K1T389
S6K1
Actin
LV-shLuc-GFP
LV-shTsc2-GFP
LV-shSCR
LV-shTsc2
pS6S240/244 / S6 [Fold of Control]
LV-shGlc-GFP
LV-shTsc2-GFP
LV-shSCR
LV-shTsc2
pS6K1T389 / S6K1 [Fold of Control]
B.
DIV18-21
Mitotracker Deep Red Intensity [% Control]
C.
Relative Cell Size [%, FSC-A]
D.
mRNA [Fold Change]
PGC1α
NRF1
mtTFA
COX-II
COX-IV
CTRL
Tsc2-KD
E.
Cell Body
Mitochondrial size [µm]
Mitochondrial shape (Circularity)
Network Branching Index
CTRL
Tsc2-KD
F.
LV-shLuc-GFP / mito-dsRed
LV-shTsc2-GFP / mito-dsRed
LV-shTsc2-GFP + TSC2-FLAG / mito-dsRed
Mitochondrial size [µm]
Mitochondrial shape (Circularity)
Number of Mitochondria [per 100µm Axon]
ns
CTRL
Tsc2-KD
Tsc2-KD +TSC2-FLAG

Figure S1. Related to Figure 1.

(A) Quantification of the levels of phosphorylated S6 protein (at Serine 240/244) and phosphorylated S6K1 (at Threonine 389) by western blotting in whole cell lysates from cortical neurons (DIV7/8) expressing shLuc-GFP, shTsc2-GFP, shSCR or shTsc2. Total levels of S6 and S6K1 are used as loading controls (n=6 experiments).

(B) Flow cytometry-based quantification of mitochondrial content using MitoTracker Deep Red staining (Mauro-Lizcano et al., 2015) in *Tsc2*-deficient cortical neurons and controls (DIV18-21). Note that this assay primarily quantifies the mitochondrial content in cell bodies since neurites may be lost during sample preparation ($n=3x10^6$ recorded events from 3 experiments).

(C) Quantification of the relative cell size in *Tsc2*-deficient cortical neurons and controls (DIV11) using flow cytometry ($n=3x10^6$ recorded events from 3 experiments).

(D) Quantification of the mRNA levels of several genes involved in regulating mitochondrial biogenesis using RT-qPCR (normalized to *Gapdh*). Graph shows the fold change (n=4-6 experiments).

(E) Quantitative assessment of mitochondrial morphology (Feret's diameter, circularity, and network branching index [$(perimeter^2)/(4\pi \times area)$] (Burbulla et al., 2010) in cell bodies of hippocampal neurons (DIV7/8, n>50 neurons from ≥3 experiments).

(F) Quantitative assessment of mitochondrial morphology (Feret's diameter and circularity) in axons of hippocampal neurons expressing shLuc-GFP, shTsc2, or shTsc2 and an shTsc2-resistant human TSC2-FLAG (DIV7/8, n>400 mitochondria from 3 experiments). Scale bar, 10µm

Luc = luciferase, SCR = scramble; *p<0.05, **p<0.01, ****<p.0001.

Figure S2.

A.

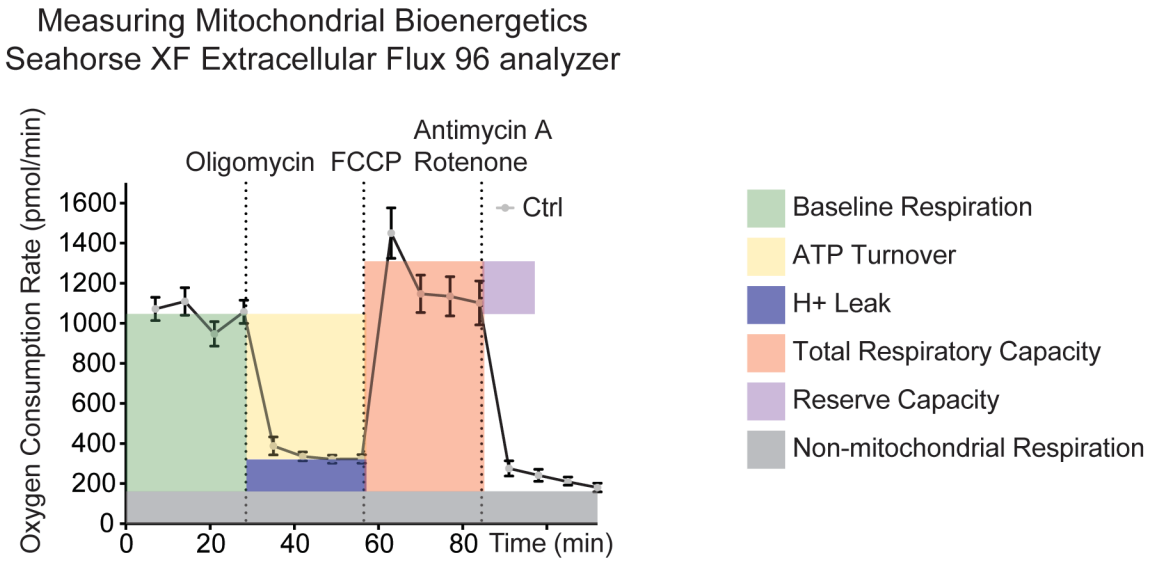

B.

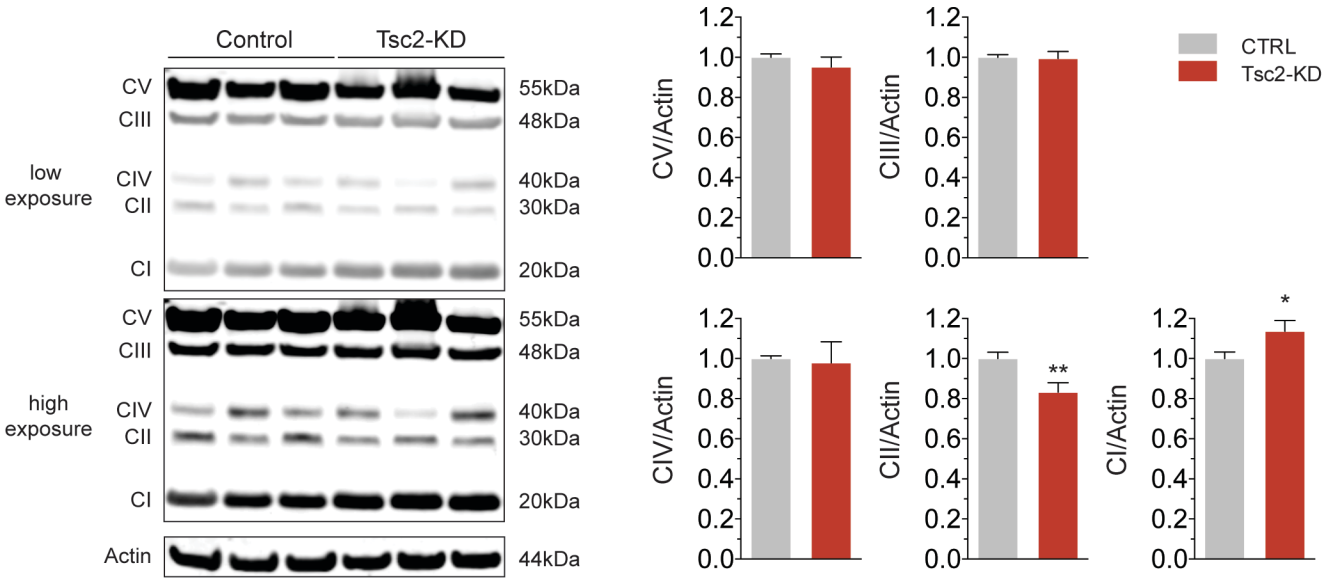

CV: ATP synthase subunit alpha
CIV: Complex IV subunit I
CIII: Complex III subunit Core 2
CII: Complex II subunit 30kDa
CI: Complex I subunit NDUFB8

Figure S2. Related to Figure 2.

(A) Schematic explaining the Seahorse XF Extracellular Flux 96 analyzer. The standardized and sequential addition of respiratory chain inhibitors allows investigating several domains of mitochondrial respiration.

(B) Quantification of different complexes of the electron transport chain (CI subunit NDUFB8, CII subunit 30kDa, CIII Core protein 2, CIV subunit I and CV alpha subunit) by western blotting in Tsc2-deficient cortical neurons and controls (DIV14, n=14 experiments).

*p<0.05, **p<0.01

Figure S3.

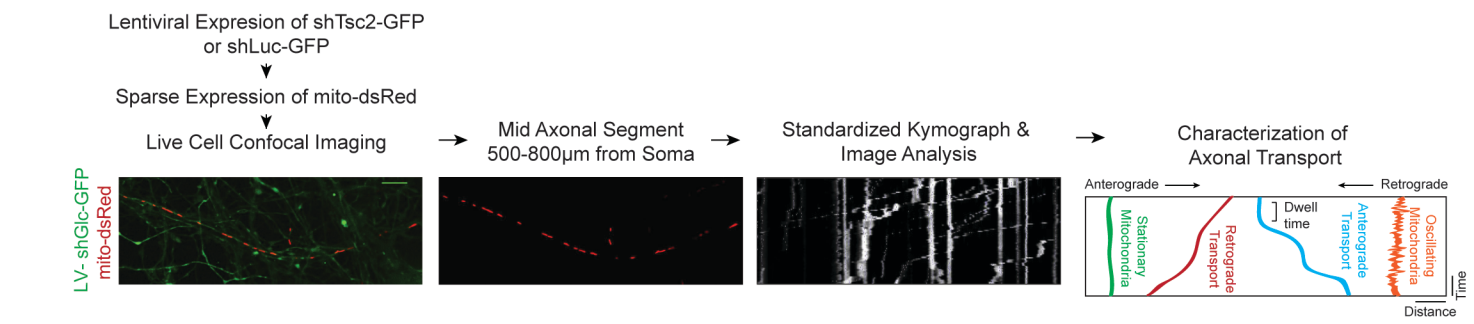
A.
Lentiviral Expresion of shTsc2-GFP or shLuc-GFP
Sparse Expression of mito-dsRed
Live Cell Confocal Imaging
Mid Axonal Segment 500-800µm from Soma
Standardized Kymograph & Image Analysis
Characterization of Axonal Transport
LV- shGlc-GFP mito-dsRed
Anterograde
Retrograde
Stationary Mitochondria
Retrograde Transport
Dwell time
Anterograde Transport
Oscillating Mitochondria
Time
Distance

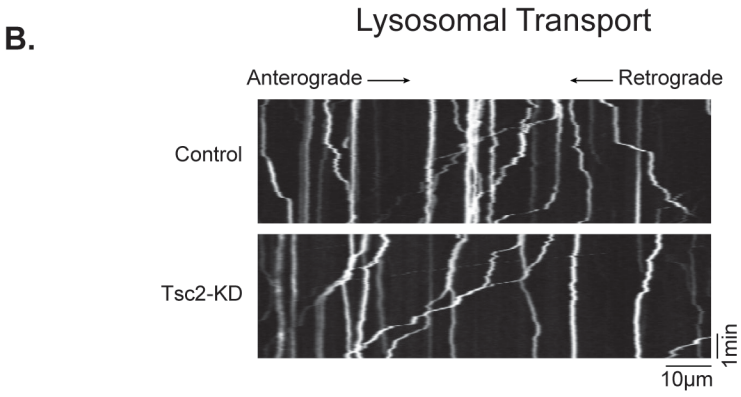
B.
Lysosomal Transport
Anterograde
Retrograde
Control
Tsc2-KD
1min
10µm

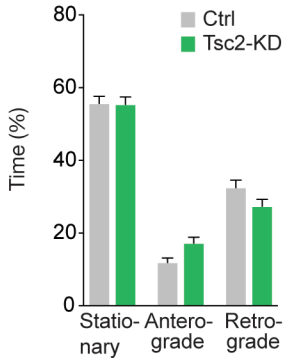
Ctrl
Tsc2-KD
Time (%)
0
20
40
60
80
Statio-nary
Antero-grade
Retro-grade

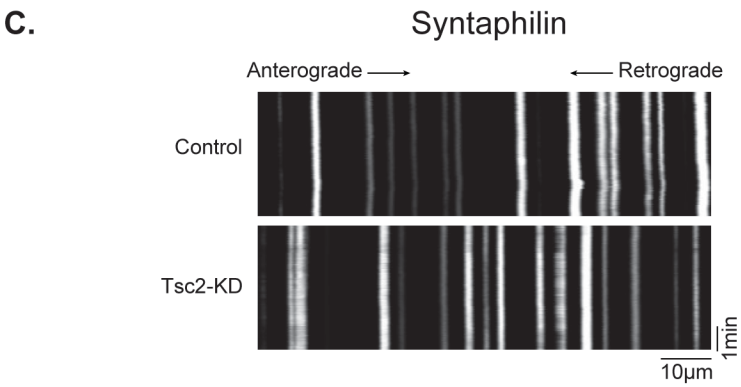
C.
Syntaphilin
Anterograde
Retrograde
Control
Tsc2-KD
1min
10µm

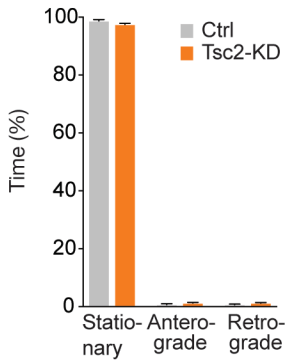
Ctrl
Tsc2-KD
Time (%)
0
20
40
60
80
100
Statio-nary
Antero-grade
Retro-grade

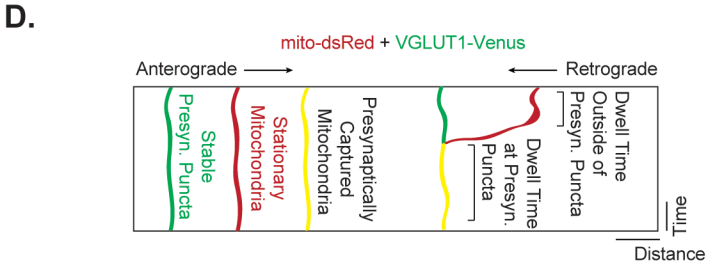
D.
mito-dsRed + VGLUT1-Venus
Anterograde
Retrograde
Stable Presyn. Puncta
Stationary Mitochondria
Presynaptically Captured Mitochondria
Dwell Time at Presyn. Puncta
Dwell Time Outside of Presyn. Puncta
Time
Distance

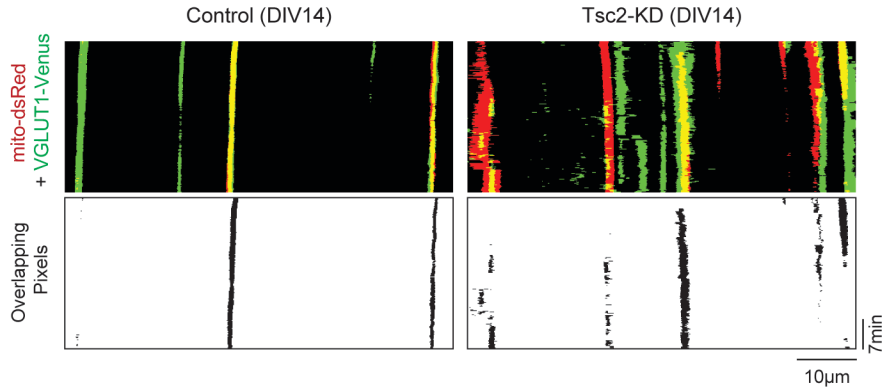
Control (DIV14)
Tsc2-KD (DIV14)
mito-dsRed + VGLUT1-Venus
Overlapping Pixels
7min
10µm

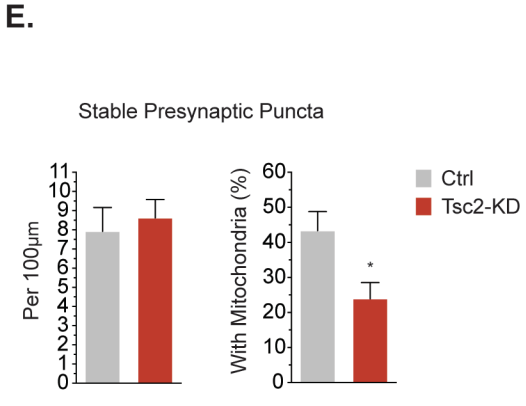
E.
Stable Presynaptic Puncta
Per 100µm
With Mitochondria (%)
Ctrl
Tsc2-KD
*

Figure S3. Related to Figure 3.

(A) Workflow and experimental setup for a standardized investigation of axonal transport in cultured neurons. Axonal transport is quantified from kymographs (Pekkurnaz et al., 2014) using a standardized protocol. Also see Supplemental Video 1 & 2.

(B) Transport of lysosomes in the mid axon (500-800µm from the cell body) of *Tsc2*-deficient hippocampal neurons and controls (DIV7/8). Graph shows the percentage of the time that lysosomes spend in a stationary position, or moving in the retrograde or anterograde direction (n>230 lysosomes from 10-12 experiments).

(C) Mitochondrial transport in the mid axon (500-800µm from the cell body) of *Tsc2*-deficient hippocampal neurons and controls (DIV7/8) overexpressing EGFP-syntaphilin. Graph shows the percentage of the time that mitochondria spend in a stationary position, or moving in the retrograde or anterograde direction (n>60 mitochondria from 4-5 experiments).

(D) Schematic exemplifying the quantitative assessment of mitochondrial capturing at presynaptic sites and representative examples in *Tsc2*-deficient hippocampal neurons and controls (DIV14/15).

(E) Quantification of the number of stable presynaptic puncta (labeled with VGLUT1-Venus and stationary for at least 30min during a 35min recording) per 100µm axon and the percentage of stable presynaptic puncta supported by stationary mitochondria in *Tsc2*-deficient hippocampal neurons and controls (DIV14/15, n=13 (Tsc2-KD), 10 (Ctrl) axons from 5-7 experiments).

Figure S4.

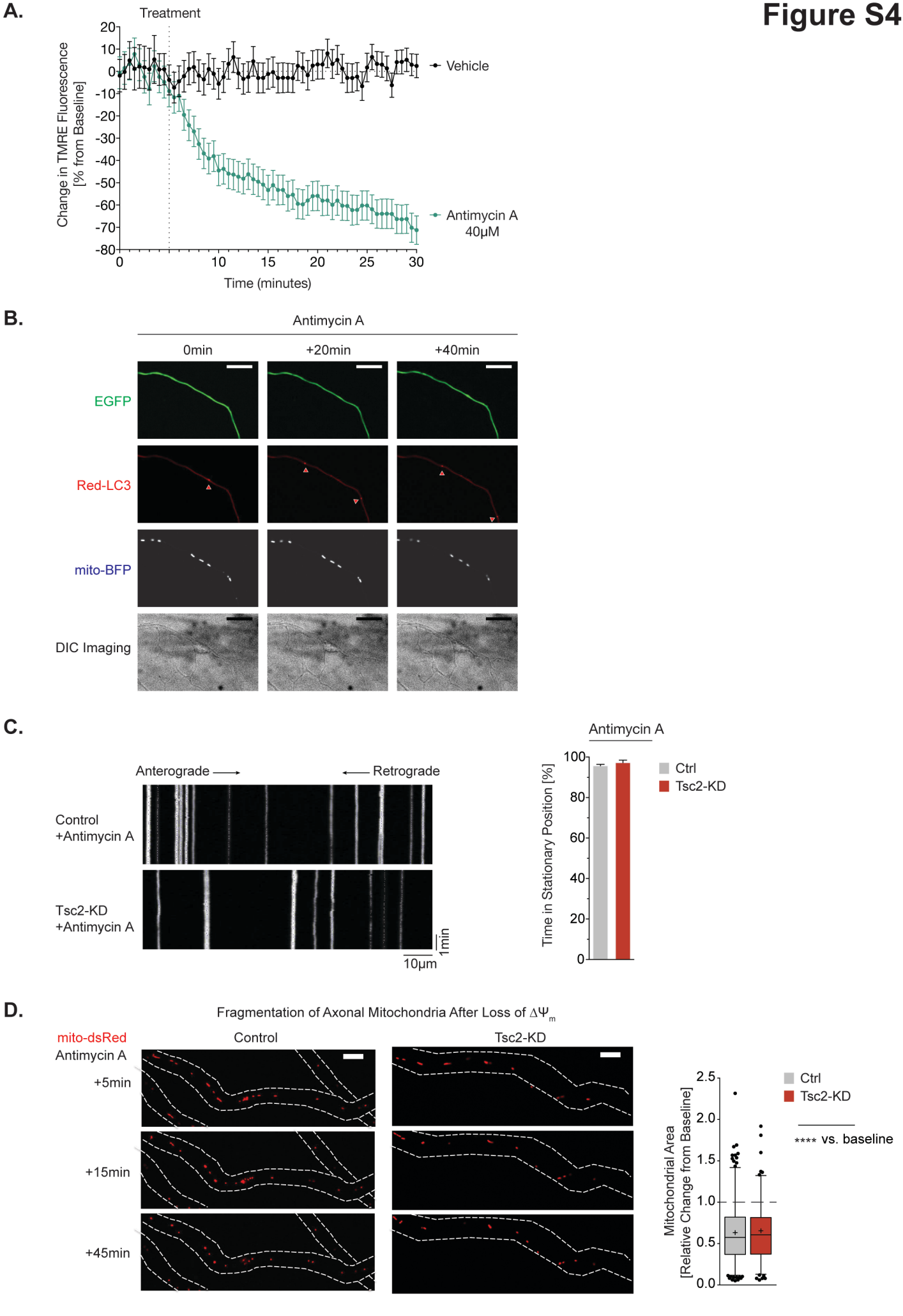
A.
Treatment
Change in TMRE Fluorescence [% from Baseline]
Time (minutes)
Vehicle
Antimycin A 40μM
B.
Antimycin A
0min
+20min
+40min
EGFP
Red-LC3
mito-BFP
DIC Imaging
C.
Anterograde
Retrograde
Control +Antimycin A
Tsc2-KD +Antimycin A
1min
10μm
Antimycin A
Time in Stationary Position [%]
Ctrl
Tsc2-KD
D.
Fragmentation of Axonal Mitochondria After Loss of ΔΨm
mito-dsRed
Antimycin A
Control
Tsc2-KD
+5min
+15min
+45min
Mitochondrial Area [Relative Change from Baseline]
Ctrl
Tsc2-KD
**** vs. baseline

Figure S4. Related to Figure 4.

(A) Graph shows the change in TMRE fluorescence from baseline (time = 0min, %). After a five-minute calibration period, antimycin A (40μM) or vehicle were applied, and TMRE fluorescence was measured every minute for a total of 30min.

(B) Representative images of a mid axon in primary hippocampal neurons (DIV7/8) expressing EGFP, Red-LC3 and mito-BFP. Red-LC3 vesicle (red arrows) accumulates at or around mitochondria following treatment with antimycin A (40μM). This is likely not an artifact as a result of possible local axon swelling because cytoplasmic EGFP does not accumulate in the vicinity of mitochondria after antimycin A treatment. DIC imaging confirms the absence of axonal swelling. Scale bar, 10μm

(C) Mitochondrial transport in the mid axon (500-800μm from the cell body) of *Tsc2*-deficient hippocampal neurons and controls (DIV7/8) acutely treated with antimycin A (40μM). Graph shows the time that mitochondria spend in a stationary position (n>100 mitochondria from 4-5 experiments). Also see Supplemental Video 3.

(D) Representative images of axonal mitochondria in time-lapse experiments in *Tsc2*-deficient hippocampal neurons and controls (DIV7/8) before and after acute $\Delta\Psi_m$-depolarization with antimycin A (40μM). Quantitative assessment of mitochondrial area after depolarization compared to baseline (n>140 mitochondria per condition from 5 experiments). Also see Supplemental Video 3. Scale bar, 5μm

****<p.0001

Figure S5.

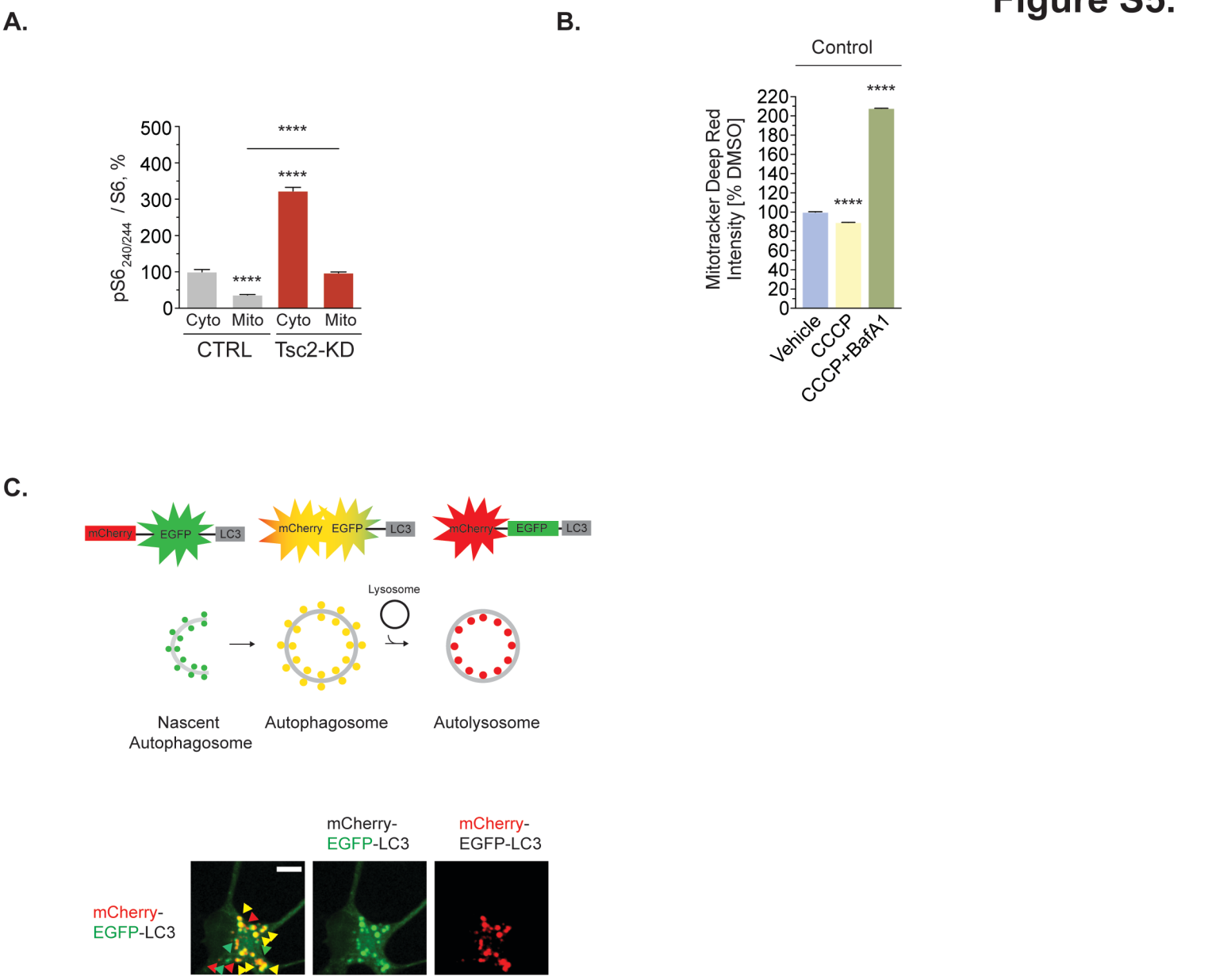

Figure S5. Related to Figures 5 & 6.

(A) Quantification of levels of phosphorylated S6 protein (at Serine 240/244) by western blotting in cytosolic and mitochondria-enriched fractions from Tsc2-deficient cortical neurons and controls (DIV7/8, see Fig. 5A). S6 was used as a loading control (n=12 experiments). Mean intensity ± SEM are shown normalized to cytosolic control condition.

(B) Flow cytometry-based quantification of mitochondrial content using MitoTracker Deep Red staining (Mauro-Lizcano et al., 2015) in neurons (DIV11) treated with CCCP (1μM, 24hr) or a combination of CCCP (1μM) and bafilomycin A1 (200nM, 24hr). Note that this assay primarily quantifies the mitochondrial content in cell bodies since neurites may be lost during sample preparation (n=2x106 recorded events per condition from 2 experiments).

(C) Schematic and representative images illustrating the mCherry-EGFP-LC3 assay (Klionsky et al., 2016; Pankiv et al., 2007). Arrowheads point to nascent autophagosomes (green), autophagosomes (yellow) and autolysosomes (red).

****<p.0001

Figure S6.

A.

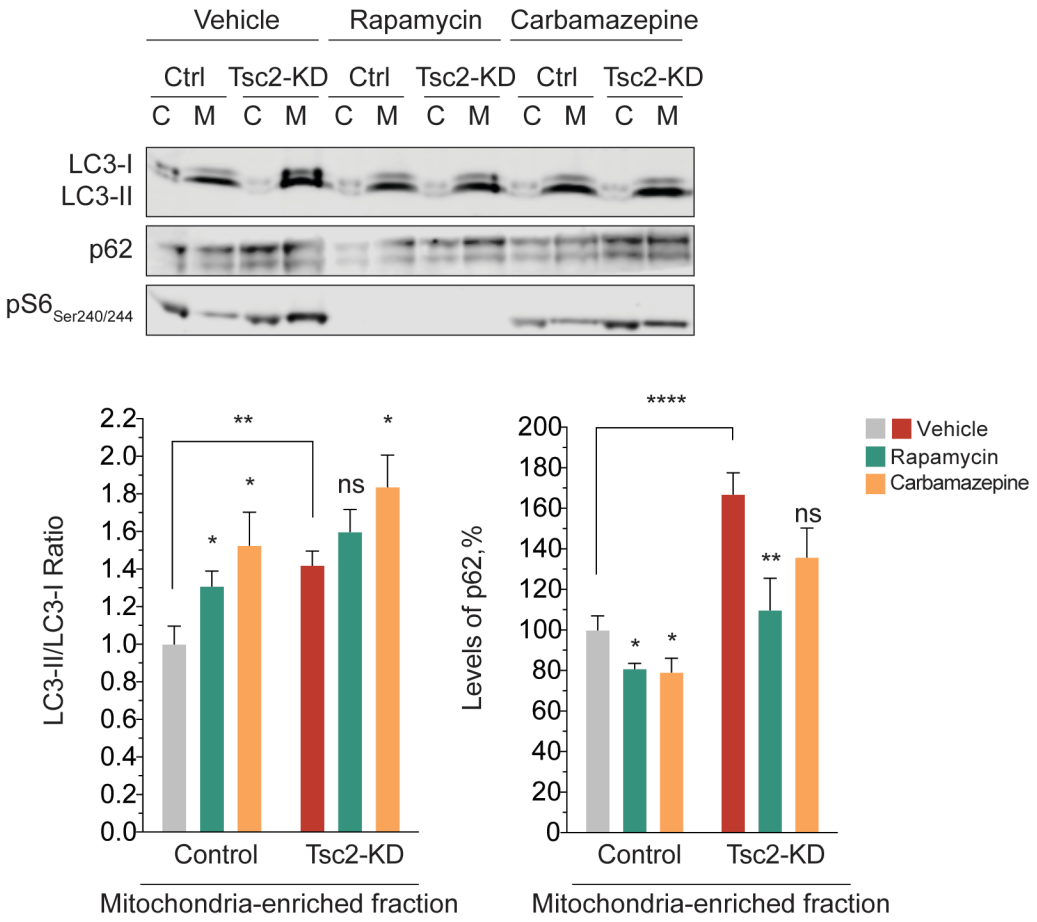

B.

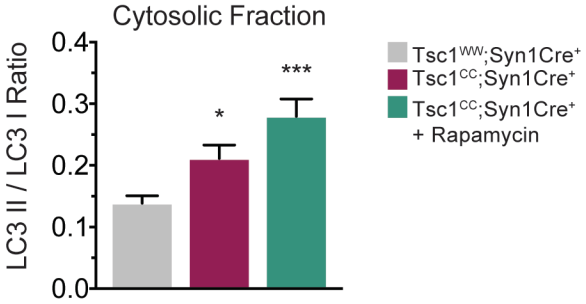

C.

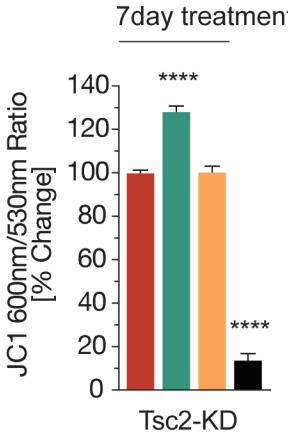

D.

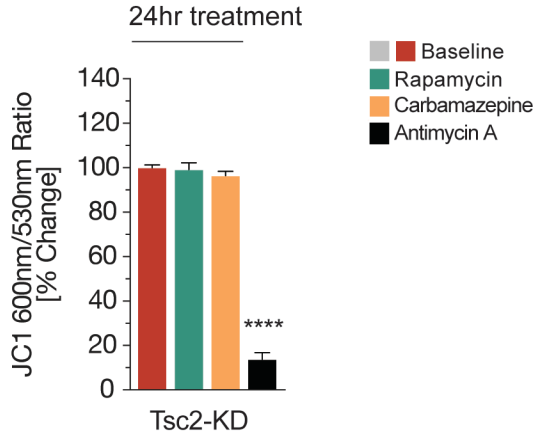

Figure S6. Related to Figure 7.

(A) Quantification of LC3-I, LC3-II, p62 and phosphorylated S6 protein (at Serine 240/244) by western blotting in cytosolic and mitochondria-enriched fractions from *Tsc2*-deficient cortical neurons and controls (DIV7/8) treated with rapamycin (20nm, 24hr), carbamazepine (100μM, 24hr) or vehicle. Graphs show the levels of LC3-II as a ratio of LC3-I, and levels of p62 in mitochondria-enriched fractions (n=12 experiments).

(B) Quantification of LC3-I and LC3-II levels by western blotting in cytosolic fractions from cortex of $Tsc1^{cc};Syn1Cre^{+}$ mice (n=8), $Tsc1^{cc};Syn1Cre^{+}$ mice treated with rapamycin (n=4), and $Tsc1^{ww};Syn1Cre^{+}$ littermate controls (n=8). Cortices were harvested on postnatal day 21.

(C and D) Approximating the $\Delta\Psi_m$ using the indicator JC1 in *Tsc2*-deficient hippocampal neurons (DIV8) treated with rapamycin (20nm) or carbamazepine (100μM) every other day for 7 days (C) or a single dose for 24 hours (D). JC-1 accumulates in mitochondria in a $\Delta\Psi_m$-dependent manner, where it exists as monomers at low concentrations (emission 530nm; green fluorescence) and forms aggregates at higher concentrations (emission 600nm; red fluorescence). Antimycin (40μM) was added for 1hr (n=3-6 experiments per condition)

C = cytosolic fraction, M = mitochondrial fraction; *p<0.05, **p<0.01, ***p<0.001, ****<p.0001

Supplemental Video 1 & 2. Examples of Mitochondrial Transport Studies
Mito-dsRed labeled mitochondria in an axon of hippocampal neurons (DIV7/8) transduced with shLuc-GFP. Nuclei are stained with NucBlue. π=15X

Supplemental Video 3. Mitochondrial Transport Following Acute $\Delta\Psi_m$-Depolarization
Mito-dsRed labeled mitochondria in an axon of a *Tsc2*-deficient hippocampal neuron (DIV7/8) acutely treated with antimycin A (40μM). $\Delta\Psi_m$-depolarization arrests mitochondrial transport and rapidly induced morphology changes indicative of mitochondrial fragmentation. π=150X; Scale bar, 10μm

Supplemental Video 4 & 5. Dynamics of Autophagosome Formation and Recruitment Following Acute $\Delta\Psi_m$-Depolarization
Autophagosome formation and recruitment in *Tsc2*-deficient hippocampal neurons and controls (DIV7/8) acutely treated with antimycin A (40μM, after 2min). Autophagosomes are labeled with LC3-Venus. π=120X; Scale bar, 10μm

Sample ID	TSC1 / TSC2 Genotype	Relation-ship	Sex	Clinical Description	Sample Source
mutTSC2 #1 (het) LAM-77	*TSC2* +/- (Heterozygous 18bp microdeletion in exon 41)	Patient	F	TSC, epilepsy	Blood
mutTSC2 #1 Control LAM-78	*TSC2* +/+ (wild type)	Father	M	Unaffected	Blood
mutTSC2 #1 (hom) LAM-77-1	*TSC2* -/- (Homozygous 18bp microdeletion in exon 41 / 8bp deletion in exon 42)	modified from LAM77	F	n.a.	Blood
mutTSC2 #2 SAH0047-01	*TSC2* +/- (c.755insA)	Patient	M	TSC, epilepsy, ASD	Fibroblasts from skin punch biopsy
mutTSC2 #2 Control SAH0047-02	*TSC2* +/+ (wild type)	Mother	F	Unaffected	Fibroblasts from skin punch biopsy

Supplemental Table 1. Table describing the demographic, clinical and genetic characteristics of donors for each of the iPSC lines used for neuronal differentiation. ASD = autism spectrum disorder, F = female, M = male, TSC = Tuberous Sclerosis Complex.

SUPPLEMENTAL EXPERIMENTAL PROCEDURES

Animals

Sprague-Dawley rats were obtained from Charles River Laboratories. *Tsc1^{ww};Syn1Cre^{+}* and *Tsc1^{cc};Syn1Cre^{+}* mice (Meikle et al., 2008; Meikle et al., 2007) were held in a light-dark cycle, temperature and humidity controlled animal vivarium with *ad libitum* food and water. All animal procedures were in accordance with the Guide for the Humane Use and Care of Laboratory Animals, and approved by the Animal Care and Use Committee at Boston Children's Hospital.

Antibodies, Reagents and Constructs

For western blotting the following antibodies were used: anti-LC3 (1:1000, Novus Cat# NB100-2220 RRID:AB_10003146), anti-p62/SQSTM1 (1:1000, Sigma-Aldrich Cat# P0067 RRID:AB_1841064), anti-PINK1 (1:1000, Abcam Cat# ab23707 RRID:AB_447627), anti-Parkin (1:1000, Abcam Cat# ab77924 RRID:AB_1566559), anti-Ubiquitin (1:2000, Millipore Cat# MAB1510 RRID:AB_2180556), anti-pS6$_{Ser240/244}$ (1:2000, Cell Signaling Technology Cat# 5364L RRID:AB_10695727), anti-S6 (1:1000, Cell Signaling Technology Cat# 2317 RRID:AB_2238583), anti-Tomm20 (1:2000, Santa Cruz Biotechnology Cat# sc-11415 RRID:AB_2207533; Abcam Cat# ab56783 RRID:AB_945896), anti-PDHE1α (1:2000, Abcam Cat# ab110334 RRID:AB_10866116), anti-Akt (1:1000, Cell Signaling Technology Cat# 4691S RRID:AB_915783), anti-GAPDH (1:2000, Santa Cruz Biotechnology Cat# sc-32233 RRID:AB_627679), anti-Total OXPHOS Rodent WB Antibody Cocktail (1:2000, Abcam Cat# ab110413). Near infrared fluorescent-labeled secondary antibodies (IR800CW, IR680LT; LI-COR Biosciences) were used for developing western blots. Oligomycin, FCCP, CCCP, rotenone, and carbamazepine were obtained from Sigma-Aldrich; rapamycin and bafilomycin A1 were purchased from LC Laboratories; and antimycin A from Enzo Life Sciences. Tetramethylrhodamine Ethyl Ester Perchlorate (TMRE), JC-1 Dye (Mitochondrial Membrane Potential Probe), NucBlue® Live ReadyProbes® Reagent, LysoTracker® Green, LysoTracker® Deep Red, and MitoTracker® Deep Red were purchased from Thermo Fisher Scientific. The following constructs were used: LV-shTsc2-GFP, LV-shTsc2, LV-shLuciferase-GFP, (described in (Nie et al., 2015; Nie and Sahin, 2012)), LV-shScramble (gift from D. Sabatini, Addgene plasmid # 1864, (Sarbassov et al., 2005)), pDsRed-Mito (gift from T. Schwarz, Boston Children's Hospital, Boston, MA), mito-BFP (gift from G. Voeltz, Addgene plasmid # 49151, (Friedman et al., 2011)) VGLUT1-Venus and EGFP-SyntaphilinFL (Courchet et al., 2013), Venus-LC3 (gift from N. Mizushima, Addgene plasmid # 38195, (Hara et al., 2008)), Red-LC3 (Di Nardo et al., 2014), mCherry-EGFP-LC3B (gift from J. Debnath, Addgene plasmid # 22418, (N'Diaye et al., 2009)), pEGFP-N1 (Clontech), human Flag–TSC2 (Zhang et al., 2013a), pCXLE-hOCT3/4-shp53-F, pCXLE-hSK, pCXLE-hUL (gift from S. Yamanaka, Addgene plasmids # 27077, # 27078, # 27080 , (Okita et al., 2011)). Ngn2 lentivirus was a kind gift from T. Südhof, Stanford University, Stanford, CA. Plasmids were subcloned into mammalian expression vectors where applicable before being purified and amplified using the Qiagen Plasmid Maxi kit according to the manufacturer's instructions. Lentivirus was produced as described in (Nie and Sahin, 2012).

Primary Neuronal Culture, Transduction and Transfection

Dissociated E18.5 rat hippocampal and cortical neurons were obtained and cultured as previously described (Nie and Sahin, 2012). In brief, rats were euthanized with CO_2 and embryos were recovered. Hippocampi and cortices were dissected and placed in chilled dissociation medium (Ca^{2+}-free HBSS with 100mM MgCl2, 10mM kynurenic acid (Sigma-Aldrich), and 100mM HEPES). Following enzymatic dissociated with papain (Worthington Biochemical Corporation) and L-cysteine (Sigma-Aldrich), trypsin inhibitor (Sigma-Aldrich) was added, and cell clumps were dissolved by trituration. Neurons were suspended in Neurobasal medium supplemented with B27, L-glutamine, and penicillin/streptomycin/primocin, and plated at a density of $1x10^6$ per well in 6-well plates, $8x10^6$ per 10cm dish, or at $2.5x10^5$ – $7.5x10^5$ per 35mm glass-bottom dishes (MatTek Corporation) coated overnight with 20µg/ml poly-D-lysine (Sigma-Aldrich) and 3.5µg/ml laminin. At 2 days in vitro (DIV), neurons were infected with lentiviral vectors in the presence of polybrene. Neurons were transfected using Lipofectamine LTX according to the manufacturer's instructions and subjected to experiments 48-72hrs later. Unless stated otherwise, all reagents were purchased from Thermo Fisher Scientific.

Generation of Human iPSC and Cortical Neuron Differentiation

Generation of Patient-derived iPSC

The IRB protocol for all experiments concerning human iPSCs was approved by Boston Children's Hospital (IRB#: 09-08-0442). Human iPSCs were generated using episomal plasmids to introduce the reprogramming factors (Oct4, Sox2, Klf4, and L-Myc) into patient derived blood cells (mutTsc2 #1, generated by LAM Therapeutics, Guilford, CT) or fibroblasts (mutTsc2 #2) and their respective control cell lines (Fig. S2B). In addition, *TSC2* homozygous mutant iPSC lines were generated from mutTsc2 #1 using TALEN-mediated mutagenesis. Heterozygous and homozygous (null) TSC2 mutations were verified through genome sequencing. Characteristics of all cell lines are summarized in Fig. S2B. ES-like colonies formed after three weeks of transfection of episomal plasmids. The observed ES-like colonies were picked manually and transferred onto mouse embryonic fibroblast feeder cells to generate iPSC lines. iPSCs were maintained on feeder cells (Globalstem) in ES media (DMEM), supplemented with 2mM L-glutamine, 1mM β-mercaptoethanol, 1x non-essential amino acids (NEAA), 20% knockout serum replacement (KOSR) and 10ng/mL basic fibroblast growth factor (bFGF). Established iPSCs were transferred to Geltrex™ LDEV-Free hESC-qualified Reduced Growth Factor Basement Membrane Matrix coated plates and maintained in STEMPRO® hESC SFM (Human Embryonic Stem Cell Culture Medium). iPSCs were passaged using dispase. All iPSCs showed normal karyotypes and passed pluripotency marker quality control analyses. All reagents were purchased from Thermo Fisher Scientific unless noted otherwise.

Cortical Neuron Differentiation

The protocol for differentiation into cortical neurons was adapted from previously published protocols (Zhang et al., 2013b). In brief, human iPSCs were dissociated into single cells with accutase and seeded on Geltrex-coated 6-well plates. For neuronal differentiation, concentrated Ngn2 lentivirus was added to iPSCs in the presence of polybrene. To express Ngn2 and for selection, doxycycline (2ug/mL) and puromycin were added following transduction with growth factors such as BDNF (10ng/mL), NT3 (10ng/mL), and laminin (0.2mg/L) in N2 media. Cells were fed every other day with BDNF (10ng/mL), NT3 (10ng/mL), and laminin (0.2mg/L), and doxycycline (2ug/mL) in B27 media for 6 days. Differentiated neuronal cells were detected by GFP expression using an EVOS microscope. All reagents were purchased from Thermo Fisher Scientific.

Drug Treatment and Tissue Recovery in *Tsc1^{ww};Syn1Cre^{+}* and *Tsc1^{cc};Syn1Cre^{+}* mice

Rapamycin was administered as described previously (Meikle et al., 2008; Tsai et al., 2013; Tsai et al., 2012). In brief, rapamycin was dissolved in 0.25% polyethylene glycol and 0.25% Tween before usage. Vehicle or rapamycin was administered intraperitoneally every two days, with rapamycin dosed at 6 mg/kg^{-1} per injection every other day starting at postnatal day 7. Cortical sections were retrieved using a Leica vibratome as described previously (Ebrahimi-Fakhari et al., 2011; Unni et al., 2011). Following homogenization using a Douce homogenizer, mitochondria-enriched and cytosolic fractions were retrieved using the Mitochondria Isolation Kit for Tissue (Thermo Fisher Scientific) similar to the approach for cultured cells described below.

RNA Isolation and RT-qPCR

RNA isolation and RT-qPCR were performed as described previously (Di Nardo et al., 2014). Total RNA was prepared using the RNAeasy KIT (Qiagen) following the manufacturer's instructions and quantified by spectrophotometry. A total of 1µg of polyA mRNA was used for reverse transcription using the SuperScript RT system (Thermo Fisher Scientific). Real time PCRs were performed using SYBG Green PCR master mix (Applied Biosystem). All PCR reactions were performed in triplicates and normalized against *Gapdh*. Analysis was performed using 7300 System SDS Software on a 7300 Real Time PCR System. The following primers were used:

	Forward Primer	Reverse Primer
Pgc1α	TATGGAGTGACATAGAGTGTGCT	CCACTTCAATCCACCCAGAAAG
Nrf1	CCCTACTCACCCAGTCAGTATG	CATCGTGCGAGGAATGAGGA
mtTFA	TGGGAGTGTTGTGAAGAGTGA	CCCAATCCCAATGACAACTC
COX-II	ACACAAGCACAATAGACGC	GTGACTGTAGCTTGGTTTAGG
COX-IV	TGGGAGTGTTGTGAAGAGTGA	GCAGTGAAGCCGATGAAGAAC

Mitochondria Isolation, Fractionation and Western Blotting

Mitochondria were isolated using the Mitochondria Isolation Kit for Cultured Cells (Thermo Fisher Scientific) with minor modifications to the protocol. In brief, cells were washed, collected and pelleted in ice-cold PBS. The supernatant was removed and cells were incubated with Reagent A buffer supplemented with protease and phosphatase inhibitors (Roche) for 2min on ice. Reagent B was added and samples were briefly vortexed, followed by incubation for 5min on ice. Reagent C was added, and samples were gently inverted. Samples were then centrifuged at 700xg for 10min at 4°C. The resulting supernatant was collected and subjected to centrifugation at 12.000xg for 15min at 4°C. The resulting supernatant contains the "cytosolic fraction". The resulting pellet contains a mitochondria-enriched fraction. Following several washes, pellets were lysed with urea lysis buffer (9M urea, 2% CHAPS in TrisBuffer, pH 8.0). This yields the "mitochondrial fraction". Western blotting was done as described in (Ebrahimi-Fakhari et al., 2011). In brief, total protein concentration was determined using the BCA Protein Assay Kit (Thermo Fisher Scientific). Equal amounts of protein were solubilized in LDS (lithium dodecyl sulfate) buffer under reducing conditions, separated by gel electrophoresis, using 4 –12% Bis-Tris gels and MOPS (3-(N-morpholino)propanesulfonic acid) or MES (2-(N-morpholino)ethanesulfonic acid) buffer (Thermo Fisher Scientific) and transferred to a PVDF membrane (EMD Millipore). Following blocking with blocking buffer (LI-COR Biosciences), membranes were incubated overnight with the respective primary antibody. Near infrared fluorescent-labeled secondary antibodies (1:5000; IR800CW, IR680LT; LI-COR Biosciences) were used and quantification was done using the Odyssey infrared imaging system and Image Studio Software (LI-COR Biosciences).

Mitochondrial Respiration Assay

Mitochondrial respiration in live intact neurons was measured using the Seahorse XF Extracellular Flux 96 analyzer with the XF Cell Mito Stress Test Kit according to the manufacturer's instructions (Seahorse Bioscience) (Ribeiro et al., 2015). In brief, oxygen consumption rate (OCR) was measured in intact cells, seeded at equal numbers and sequentially exposed to control assay medium, oligomycin (ATP synthase inhibitor), FCCP (collapses the proton gradient and disrupts the mitochondrial membrane potential) and a mix of rotenone (complex I inhibitor) and antimycin A (complex III inhibitor). Following the serially injection of these compounds, OCR was used to calculate different domains of mitochondrial function such as baseline respiration, ATP turnover, H^+ leak respiration, total respiratory capacity, and non-mitochondrial respiration (Fig. S2A). OCR data were normalized to DNA content on a per well basis.

TMRE and JC1 Dye Staining

To determine the mitochondrial membrane potential ($\Delta\Psi_m$) in cultured, intact neurons, we employed the potentiometric, cell-permeable fluorescent probe TMRE (tetramethylrhodamine, ethyl ester) (Joshi and Bakowska, 2011) and the mitochondrial membrane indicator dye JC1 (tetraethylbenzimidazolylcarbocyanine iodide) (Perry et al., 2011; Scaduto and Grotyohann, 1999). The fluorescent signal of TMRE is directly correlated with the mΨ across the inner mitochondrial membrane. JC1 shifts from green to red with increasing aggregation in mitochondria, thus allowing for a ratiometric, quantitative assessment of the mitochondrial polarization states. Neurons were pulse-labeled with 20nM TMRE at 37°C, 5% CO_2, for 20min and maintained in Hibernate E Low Fluorescence (BrainBits LLC) containing 5nM TMRE during subsequent live imaging experiments. Images were acquired after equilibrium was achieved. For pulse labeling with JC1, neurons were incubated with 1ug/ml of JC1 for 20min under growth conditions (37°C, 5% CO_2).

Flow Cytometry Analysis to Determine Mitochondrial Mass and Turnover

Mitochondrial mass was quantified using a flow cytometry-based assay modified from existing protocols (Mauro-Lizcano et al., 2015). Following drug treatment, neuronal cultures were washed using 1X warm PBS followed by gentle enzymatic detaching with papain (10U/ml, Worthington Biochemical Corporation) in pH-adjusted dissociation medium (10mM MgCl2, 1mM kynurenic acid (Sigma-Aldrich), 10mM HEPES in HBSS) supplemented with L-cysteine (Sigma-Aldrich). Trypsin inhibitor (Sigma-Aldrich) was added, cells were gently recovered, passed through a cell-strainer cap and collected in polypropylene round-bottom tubes (Falcon). Following another wash in trypsin-inhibitor solution, cells were re-suspended in dissociation medium containing 250nM MitoTracker Deep Red and/or DAPI and incubated for 20min at 37°C. Cells were then washed, centrifuged and re-suspended in PBS containing 2% fetal bovine serum. Flow cytometry was carried out using

the BD LSRFortessa™ cell analyzer, equipped with FACSDIVA (BD Biosciences) software and data were analyzed using FlowJo 10 software (TreeStar). For each experiment, cells were carefully gated to include only viable, GFP-positive populations in the analysis.

Live Cell Confocal Imaging and Analysis

Confocal images were obtained using a spinning disk confocal microscope (Perkin Elmer) with a Nikon Ti-Eclipse inverted live cell imaging system equipped with an electron-multiplying charge-coupled device camera (C9100; Hamamatsu Photonics) using a 60X/ 1.40 NA lens or 20X/0.75 NA lens, Perfect Focus System (Nikon) and Volocity software (PerkinElmer). During live imaging, neurons were maintained in Hybernate E medium (BrainBits LLC) at 37°C in an environmental chamber for up to 70min. Transduced neurons were identified based on their GFP fluorescence. Axons were selected based on morphologic criteria, namely their length, uniform and thin caliber, sparse branching and meandering course. Only those that appeared as single axons were chosen. All acquisition settings, including detector sensitivity and camera exposure time, were kept constant during imaging. Laser power was kept at a minimum to avoid photobleaching.

Mitochondrial Motility

To quantify characteristics of mitochondrial transport in axons of cultured rat hippocampal neurons, mitochondria were labeled by transfection with mito-DsRed. Sparsely transfected cultures allow for the tracing of individual axons and their orientation can be determined unambiguously. A mid-axonal compartment (100-150µm in length, ~500-800µm from the soma) was chosen, and images were captured every 3 seconds for 5min per axon for a maximum of 60 minutes. All acquisition settings, including detector sensitivity and camera exposure time, were set to keep the signal in a dynamic range and were kept constant during imaging. Laser power was kept at 1-2% to avoid photobleaching. To analyze the movement of individual axonal mitochondria in a standardized manner we employed the custom-written Kymolizer macro in Image J (Pekkurnaz et al., 2014) to generate kymographs of 5min long time-lapse movies and to calculate mitochondrial motility. Velocities of less than 0.05 mm/s were considered zero in order to avoid bias caused by stage drift (Wang and Schwarz, 2009). For lysosomal transport studies, lysosomes were labeled with LysoTracker Green (200nm, 30min).

Axonal Mitophagy

LC3 recruitment to depolarized axonal mitochondria was quantified as previously described (Ashrafi et al., 2014; Klionsky et al., 2016). In brief, neurons were transfected with mito-dsRed and Venus-LC3 to label mitochondria and autophagosomes respectively. A mid-axonal compartment was identified, and the number of mitochondria co-localizing with Venus-LC3–positive autophagosomes was counted before and every 5 min (≤55min) after application of antimycin A. The maximum percentage of LC3-positive mitochondria within 55min was calculated to show the percentage of LC3-labeled mitochondria after mitochondrial damage. In a similar manner LysoTracker Green was employed to label axonal lysosomes. LysoTracker Green was incubated at 200nM for 30min under growth conditions. Following a baseline image, images were acquired every 10 min (≤60min) and the maximum percentage of mitochondria co-localizing with LysoTracker Green positive vesicles was calculated.

Nascent Presynaptic Sites and Mitochondria

Mitochondrial capturing at synapses was measured as previously reported (Courchet et al., 2013). In brief, VGLUT1-Venus and mito-dsRed were sparsely expressed by transient transfection. Dual-channel time-lapse confocal microscopy was used to image mitochondria and VGLUT1 vesicles in distal axons at 0.1 frames per second for 35min. For each channel kymographs were generated using the custom-written Kymolizer macro in Image J (Pekkurnaz et al., 2014). Colocalization was assessed using the colocalization plugin in Image J and the dwell time of motile mitochondria over and outside of stable presynaptic sites was calculated using a customized macro in Image J. Similarly, the number of stable presynaptic puncta (stationary over 30min) and the proportion of stationary mitochondria (stationary over 30min) captured at stable presynaptic puncta was quantified.

mCherry-EGFP LC3 Tandem Assay

The tandem mCherry-EGFP-LC3 assay was used as previously described (Kimura et al., 2007; Pankiv et al., 2007). Autophagic vesicles before fusion with lysosomes (“yellow only”) and autolysosomes (“red only”) were quantified on a per cell body basis from time-lapse experiments using Image J (Fig. S5C).

Lysosomal Mass

LysoTracker Deep Red was incubated at 200nM for 30 min under growth conditions. NucBlue was used to stain nuclei. Using a 20X magnification and the automated stage function in Volocity, coverslips were scanned. GFP-positive neurons (expressing shTsc2 or shLuciferase respectively) were outlined and the area covered by LysoTracker Deep Red within the GFP-positive area was calculated using the co-localization plugin and a customized macro in Image J. Per condition >$25x10^3$ neurons were quantified.

Transmission Electron Microscopy

Electron microscopy was done according to standard protocols. In brief, mice were perfused with 1xPBS for 4min followed by 2% PFA, 3% glutaraldehyde and 0.03% picric acid in 0.15M cacodylate buffer, pH 7.4 for 15 minutes. Brains were removed and postfixed overnight using the same fixative. Next, samples were washed with 0.15M cacodylate buffer and stained en bloc in 2% osmium tetroxide, 1.5% ferrocyanide in cacodylate buffer for 5h, washed with water, and stained in 1% aqueous uranylacetate for 2h. Samples were dehydrated in graded alcohols and propylene oxide and embedded in TAAB 812 Resin (Canemco-Marivac). Blocks were kept at 60°C for 48hr to complete polymerization. Both semi- and ultrathin sections were prepared using a Leica EM UC7 Ultramicrotome. Digital images were taken with an AMT CCD camera mounted on a Tecnai™ G^2 Spirit BioTWIN Transmission Electron Microscope.

Statistical Analysis

Statistical analysis was performed with GraphPad Prism version 6.0 for Mac OS X (GraphPad Software, Inc.). Throughout the manuscript, the distribution of data points is expressed as mean ± standard error of the mean. Mann–Whitney U test, unpaired Student t-test or one-way ANOVA with post hoc Bonferroni's multiple-comparisons test was used to determine the significance of differences between conditions. $p<0.05$ was considered significant. p-values are denoted as follows: $p<0.05$ (*), $p<0.01$ (**), $p< 0.001$ (***), and $p< 0.0001$ (****).

REFERENCES IN SUPPLEMENTAL MATERIAL

Ashrafi, G., Schlehe, J.S., LaVoie, M.J., and Schwarz, T.L. (2014). Mitophagy of damaged mitochondria occurs locally in distal neuronal axons and requires PINK1 and Parkin. J Cell Biol *206*, 655-670.

Burbulla, L.F., Schelling, C., Kato, H., Rapaport, D., Woitalla, D., Schiesling, C., Schulte, C., Sharma, M., Illig, T., Bauer, P.*, et al.* (2010). Dissecting the role of the mitochondrial chaperone mortalin in Parkinson's disease: functional impact of disease-related variants on mitochondrial homeostasis. Hum Mol Genet *19*, 4437-4452.

Courchet, J., Lewis, T.L., Jr., Lee, S., Courchet, V., Liou, D.Y., Aizawa, S., and Polleux, F. (2013). Terminal axon branching is regulated by the LKB1-NUAK1 kinase pathway via presynaptic mitochondrial capture. Cell *153*, 1510-1525.

Di Nardo, A., Wertz, M.H., Kwiatkowski, E., Tsai, P.T., Leech, J.D., Greene-Colozzi, E., Goto, J., Dilsiz, P., Talos, D.M., Clish, C.B.*, et al.* (2014). Neuronal Tsc1/2 complex controls autophagy through AMPK-dependent regulation of ULK1. Hum Mol Genet *23*, 3865-3874.

Ebrahimi-Fakhari, D., Cantuti-Castelvetri, I., Fan, Z., Rockenstein, E., Masliah, E., Hyman, B.T., McLean, P.J., and Unni, V.K. (2011). Distinct roles in vivo for the ubiquitin-proteasome system and the autophagy-lysosomal pathway in the degradation of alpha-synuclein. J Neurosci *31*, 14508-14520.

Friedman, J.R., Lackner, L.L., West, M., DiBenedetto, J.R., Nunnari, J., and Voeltz, G.K. (2011). ER tubules mark sites of mitochondrial division. Science *334*, 358-362.

Hara, T., Takamura, A., Kishi, C., Iemura, S., Natsume, T., Guan, J.L., and Mizushima, N. (2008). FIP200, a ULK-interacting protein, is required for autophagosome formation in mammalian cells. J Cell Biol *181*, 497-510.

Joshi, D.C., and Bakowska, J.C. (2011). Determination of mitochondrial membrane potential and reactive oxygen species in live rat cortical neurons. J Vis Exp.

Kimura, S., Noda, T., and Yoshimori, T. (2007). Dissection of the autophagosome maturation process by a novel reporter protein, tandem fluorescent-tagged LC3. Autophagy *3*, 452-460.

Klionsky, D.J., Abdelmohsen, K., Abe, A., Abedin, M.J., Abeliovich, H., Acevedo Arozena, A., Adachi, H., Adams, C.M., Adams, P.D., Adeli, K.*, et al.* (2016). Guidelines for the use and interpretation of assays for monitoring autophagy (3rd edition). Autophagy *12*, 1-222.

Mauro-Lizcano, M., Esteban-Martinez, L., Seco, E., Serrano-Puebla, A., Garcia-Ledo, L., Figueiredo-Pereira, C., Vieira, H.L., and Boya, P. (2015). New method to assess mitophagy flux by flow cytometry. Autophagy *11*, 833-843.

Meikle, L., Pollizzi, K., Egnor, A., Kramvis, I., Lane, H., Sahin, M., and Kwiatkowski, D.J. (2008). Response of a neuronal model of tuberous sclerosis to mammalian target of rapamycin (mTOR) inhibitors: effects on mTORC1 and Akt signaling lead to improved survival and function. J Neurosci *28*, 5422-5432.

Meikle, L., Talos, D.M., Onda, H., Pollizzi, K., Rotenberg, A., Sahin, M., Jensen, F.E., and Kwiatkowski, D.J. (2007). A mouse model of tuberous sclerosis: neuronal loss of Tsc1 causes dysplastic and ectopic neurons, reduced myelination, seizure activity, and limited survival. J Neurosci *27*, 5546-5558.

N'Diaye, E.N., Kajihara, K.K., Hsieh, I., Morisaki, H., Debnath, J., and Brown, E.J. (2009). PLIC proteins or ubiquilins regulate autophagy-dependent cell survival during nutrient starvation. EMBO Rep *10*, 173-179.

Nie, D., Chen, Z., Ebrahimi-Fakhari, D., Di Nardo, A., Julich, K., Robson, V.K., Cheng, Y.C., Woolf, C.J., Heiman, M., and Sahin, M. (2015). The Stress-Induced Atf3-Gelsolin Cascade Underlies Dendritic Spine Deficits in Neuronal Models of Tuberous Sclerosis Complex. J Neurosci *35*, 10762-10772.

Nie, D., and Sahin, M. (2012). A genetic model to dissect the role of Tsc-mTORC1 in neuronal cultures. Methods Mol Biol *821*, 393-405.

Okita, K., Matsumura, Y., Sato, Y., Okada, A., Morizane, A., Okamoto, S., Hong, H., Nakagawa, M., Tanabe, K., Tezuka, K.*, et al.* (2011). A more efficient method to generate integration-free human iPS cells. Nat Methods *8*, 409-412.

Pankiv, S., Clausen, T.H., Lamark, T., Brech, A., Bruun, J.A., Outzen, H., Overvatn, A., Bjorkoy, G., and Johansen, T. (2007). p62/SQSTM1 binds directly to Atg8/LC3 to facilitate degradation of ubiquitinated protein aggregates by autophagy. J Biol Chem *282*, 24131-24145.

Pekkurnaz, G., Trinidad, J.C., Wang, X., Kong, D., and Schwarz, T.L. (2014). Glucose regulates mitochondrial motility via Milton modification by O-GlcNAc transferase. Cell *158*, 54-68.

Perry, S.W., Norman, J.P., Barbieri, J., Brown, E.B., and Gelbard, H.A. (2011). Mitochondrial membrane potential probes and the proton gradient: a practical usage guide. Biotechniques *50*, 98-115.

Ribeiro, S.M., Gimenez-Cassina, A., and Danial, N.N. (2015). Measurement of mitochondrial oxygen consumption rates in mouse primary neurons and astrocytes. Methods Mol Biol *1241*, 59-69.

Sarbassov, D.D., Guertin, D.A., Ali, S.M., and Sabatini, D.M. (2005). Phosphorylation and regulation of Akt/PKB by the rictor-mTOR complex. Science *307*, 1098-1101.

Scaduto, R.C., Jr., and Grotyohann, L.W. (1999). Measurement of mitochondrial membrane potential using fluorescent rhodamine derivatives. Biophys J *76*, 469-477.

Tsai, P.T., Greene-Colozzi, E., Goto, J., Anderl, S., Kwiatkowski, D.J., and Sahin, M. (2013). Prenatal rapamycin results in early and late behavioral abnormalities in wildtype C57BL/6 mice. Behav Genet *43*, 51-59.

Tsai, P.T., Hull, C., Chu, Y., Greene-Colozzi, E., Sadowski, A.R., Leech, J.M., Steinberg, J., Crawley, J.N., Regehr, W.G., and Sahin, M. (2012). Autistic-like behaviour and cerebellar dysfunction in Purkinje cell Tsc1 mutant mice. Nature *488*, 647-651.

Unni, V.K., Ebrahimi-Fakhari, D., Vanderburg, C.R., McLean, P.J., and Hyman, B.T. (2011). Studying protein degradation pathways in vivo using a cranial window-based approach. Methods *53*, 194-200.

Wang, X., and Schwarz, T.L. (2009). The mechanism of Ca2+ -dependent regulation of kinesin-mediated mitochondrial motility. Cell *136*, 163-174.

Zhang, J., Kim, J., Alexander, A., Cai, S., Tripathi, D.N., Dere, R., Tee, A.R., Tait-Mulder, J., Di Nardo, A., Han, J.M.*, et al.* (2013a). A tuberous sclerosis complex signalling node at the peroxisome regulates mTORC1 and autophagy in response to ROS. Nat Cell Biol *15*, 1186-1196.

Zhang, Y., Pak, C., Han, Y., Ahlenius, H., Zhang, Z., Chanda, S., Marro, S., Patzke, C., Acuna, C., Covy, J.*, et al.* (2013b). Rapid single-step induction of functional neurons from human pluripotent stem cells. Neuron *78*, 785-798.